

## GAS PHASE KINETICS DURING DIAMOND GROWTH: CH<sub>4</sub> AS GROWTH SPECIES

Stephen J. Harris  
Physical Chemistry Department  
General Motors Research Labs  
Warren, MI 48090

### Introduction

There has been considerable interest in the growth of diamond thin films in recent years<sup>1,2</sup>. This interest derives from the superlative properties of diamonds: they are very hard, have a high thermal conductivity, are chemically inert, and have an extremely wide optical transmission window. In addition, single crystal diamonds have the potential for being uniquely good semiconductors<sup>2</sup>.

Unfortunately, at present we have little understanding of the chemical processes which are involved in and which control diamond nucleation and growth. This is because there have been no experiments which have simultaneously characterized both the chemical environment and the kinetics of diamond growth. Recently C<sub>2</sub>H<sub>2</sub> (acetylene)<sup>3,4</sup>, C<sub>2</sub>H<sub>4</sub> (ethylene)<sup>3</sup>, CH<sub>3</sub> (methyl radical)<sup>3</sup>, and H (atomic hydrogen)<sup>3</sup> have been detected during filament-assisted diamond growth experiments. Harris et al.<sup>4</sup> used a simple zero-dimensional chemical kinetics model to show that only CH<sub>4</sub> (methane), C<sub>2</sub>H<sub>4</sub>, C<sub>2</sub>H<sub>2</sub>, and/or CH<sub>3</sub> could be contributing significantly to surface growth in those experiments. This result is consistent with semi-empirical quantum mechanical studies of the diamond growth mechanism which suggest that the growth species is either C<sub>2</sub>H<sub>2</sub><sup>5</sup> or CH<sub>3</sub><sup>6</sup>.

Earlier detailed measurements of the kinetics of diamond growth on diamond seed crystals from CH<sub>4</sub>-H<sub>2</sub> mixtures were made by Chauhan, Angus, and Gardner<sup>7</sup>. Although the chemical species present were not determined in their work, we recognized that the gas phase chemistry could be approximately modeled based on the information that was provided. In this work we analyze the data of Chauhan et al.<sup>7</sup> to determine which species accounted for the diamond growth that was observed.

### Analysis

The experiments of Chauhan et al.<sup>7</sup> were carried out on a microbalance which allowed the rate of diamond growth to be measured. For the particular experiment that we modeled, labeled 44-C, a 0.5 torr mixture of 70% CH<sub>4</sub> and 30% H<sub>2</sub> passed through a cylindrical 2.54 cm diameter flow tube into the top of a spherical 10.16 cm diameter pyrex reaction chamber, at the center of which was suspended a crucible holding 98.934 mg of diamond seed crystals. The gases were pumped away at the bottom of the reaction chamber through a 3.81 cm diameter flow tube. The seed crystals, which had a BET surface area of 7 m<sup>2</sup>/g, were heated to 1438 K by radiation from a lamp; there were no other heaters in the system. The wall temperature of the reaction chamber was maintained below 500 K, eliminating heterogeneous pyrolysis chemistry there. The gas velocity was not specified, but Chauhan et al.<sup>7</sup> stated that the gases flowed at a rate "such that the methane available was more than 50 times that required to obtain the observed deposition rates." This implies an input flow velocity of at least 94 cm/s, readily achieved in flow tubes of this size. Chauhan et al.<sup>7</sup>

determined that all of the initial weight gain as monitored by the microbalance was due to diamond, although as time progressed more and more of the weight gain came from non-diamond (pyrolytic) carbon. In this work we model only the initial growth period, before any formation of pyrolytic carbon.

The measurements of Chauhan et al.<sup>7</sup> showed an initial fractional growth rate of

$$\frac{1}{m} \frac{dm}{dt} = 1.31 \times 10^{-3} \text{ min}^{-1}, \quad (1)$$

where  $m$  is the mass of the diamond crystals. This rate corresponds to a specific surface growth rate of  $3.1 \times 10^{-10}$  g/cm<sup>2</sup>·s. For a growth species depositing  $n_c$  carbon atoms with each reaction, Eqn. (1) implies that  $1.6 \times 10^{13}/n_c$  molecules reacted/cm<sup>2</sup>·s. This reaction rate is equal to the collision rate of growth species with the diamond surface (calculated from the kinetic theory of gases<sup>8</sup>) times the reaction probability  $R$  that a given collision leads to reaction,

$$\frac{1.6 \times 10^{13}}{n_c} = 3.52 \times 10^{22} \frac{P}{\sqrt{MT}} R, \quad (2)$$

where  $P$  is the growth species pressure in torr,  $M$  is the molecular weight of the growth species, and  $T$  is the temperature in degrees Kelvin. For  $M = 15n_c$  and  $T = 1438$  K, the growth species mole fraction is  $X = 1.3 \times 10^{-7}/R\sqrt{n_c}$ . Since  $R \leq 1$  the mole fraction for the growth species must be at least  $X_{\min} = 1 \times 10^{-7}$  (0.1 parts per million) for reasonable (i.e., small) values of  $n_c$ . This is our first constraint on the growth species.

Diamond growth acts as a sink for growth species, so in order to maintain a *steady state* concentration greater than  $X_{\min}$  the growth species must not be depleted faster than they are created and transported to the diamond seed crystals for reaction. From Eqn. (1), the diamond growth rate was  $2.2 \times 10^{-6}$  g/s, all of which mass must ultimately have come from  $CH_4$ . This implies that at least  $8.1 \times 10^{16}$   $CH_4$  molecules reacted per second, and that at least  $8.1 \times 10^{16}/n_c$  growth species were formed per second (unless  $CH_4$  was itself the growth species). This is our second constraint on the growth species.

We have modeled the gas phase pyrolysis chemistry in this system in order to determine which hydrocarbons satisfied these two constraints in the system of Chauhan et al.<sup>7</sup> Several approximations and assumptions were used; these are discussed in a separate section below.

The experiment is modeled as follows. We assume 1-dimensional flow so that the gas temperature and species concentrations depend only on the distance  $Z$  along the tube or reaction chamber. The gas is assumed to enter the 2.54 cm diameter flow tube at  $Z = 0$ ,  $T = 300$  K, and  $v_0 = 94$  cm/s. The gas flows into the reaction chamber at  $Z = 35.1$  cm and  $T = 500$ . Beyond that point the gas temperature is assumed to rise linearly with  $Z$  until it reaches a maximum of 1438 K at the crucible, taken to be at  $Z = 40$ . The temperature then falls slowly (heat loss to the relatively distant reaction chamber walls assumed small) to 1250 K as it exits the reaction chamber at  $Z = 44.7$ . For  $Z > 44.7$ , where the gas is again in a flow tube, the temperature drops to 500 K by  $Z = 85$  cm. The gas velocity in the system is calculated assuming that the flux is given by  $\rho v A = \text{constant}$ , where  $\rho$  is the gas density and  $A$  is the cross sectional area of the tube or reaction chamber. We estimate that  $v = 28$  cm/s at the crucible and that the gas has a residence time in the reaction chamber of 250 ms. The gas phase chemistry is modeled using the Sandia burner code<sup>9</sup> together with

the reaction mechanism shown in Table I. A similar mechanism was successful in predicting the species concentration profiles in a number of premixed flat flames<sup>10,11</sup>. Although the mechanism considers species as large as  $C_4H_6$ , only the  $C_1$  and  $C_2$  part of the mechanism is shown since the concentrations of larger species are always extremely small and since the  $C_3$  and  $C_4$  chemistry is less well known. The pressure-dependent reactions shown in the Table are in the low pressure limit. Rate constants  $k = AT^n e^{-E_a/RT}$  are given for the forward direction; rate constants for the reverse direction are calculated using thermodynamic data from the Chemkin data base<sup>12</sup>, supplemented where necessary by other standard sources<sup>13</sup>.

### Results

The predictions of the model are shown in Figure 1, which displays steady state profiles of all species that reach mole fractions of at least  $10^{-14}$ . The reaction chamber is located between  $Z = 35.1$  and  $44.7$  cm, and the crucible is located at  $Z = 40$ .

Chemical reaction is initiated in this system by the reverse of Reaction 2 of Table I (denoted  $A_{-2}$ ) which produces  $H$  and  $CH_3$  and which occurs only at the highest temperature positions near  $Z = 40$ . The  $H$  is rapidly consumed by  $A_3$ , forming additional  $CH_3$ . Within the reaction chamber the  $CH_3$  mole fraction (and the mole fractions of many other species) is nearly independent of  $Z$  because the gas velocity there is low, and mixing by diffusion is rapid. As the  $CH_3$  formed by  $A_{-2}$  and  $A_3$  diffuses upstream toward the flow tube, it is consumed by  $A_{-3}$ , creating  $H$  atoms.  $CH_3$  decay for  $Z < 35.1$  is due mainly to  $A_{-14}$ , which is nearly irreversible at the low temperatures in the flow tube.  $C_2H_6$ , formed mainly between  $Z = 33$  and  $Z = 35$  by  $A_{-14}$ , is for the most part carried downstream into the reaction chamber. However, some  $C_2H_6$  diffuses upstream against a high gas velocity, giving the falloff in concentration for  $Z < 34$ .  $C_2H_5$  (ethyl radical) is formed in the reaction chamber by both  $A_{12}$  and  $A_{13}$ , but near  $Z = 40$  it decomposes rapidly via  $A_{15}$  to make  $C_2H_4$ , accounting for the drop in the  $C_2H_5$  mole fraction there.  $A_{17}$  produces small amounts of  $C_2H_2$  at  $Z = 40$ . Some  $C_2H_4$  and  $C_2H_2$  formed there diffuse upstream into the flow tube.

Because of the low pressure (0.5 torr) and short residence time (250 ms) in the reaction chamber, the chemical reactions are far too slow for the  $CH_4/H_2$  mixture to attain equilibrium. For example, at equilibrium the mole fraction of  $C_2H_2$  at the crucible would be 0.19, thirteen orders of magnitude higher than shown in Figure 1. The equilibrium mole fractions of some other relevant species are  $X_{CH_4}^{eq} = 3.2 \times 10^{-4}$ ,  $X_H^{eq} = 2.8 \times 10^{-4}$ ,  $X_{C_2H_4}^{eq} = 4.8 \times 10^{-5}$ ,  $X_{C_2H_6}^{eq} = 3.6 \times 10^{-6}$ , and  $X_{CH_3}^{eq} = 2.7 \times 10^{-6}$ . Comparing these values to those shown in Figure 1, it is clear that the assumption of equilibrium is totally unjustified in this system. We showed previously<sup>4</sup> that the assumption of equilibrium is equally untenable during filament-assisted diamond growth. Instead, the compositions in these systems are kinetically controlled.

### Discussion

The first conclusion we draw from Figure 1 is that aside from  $CH_4$  ( $X = 0.7$ ), only  $C_2H_6$  and  $CH_3$  have mole fractions above  $X_{min} = 1 \times 10^{-7}$ . Using Eqn. (2), we can calculate the reaction probability  $R$  required if we assume that one of these species is responsible for the observed diamond growth. The result is  $R_{CH_4} \sim 10^{-7}$ , while  $R_{C_2H_6}$  and  $R_{CH_3} \sim 10^{-1}$ . To put these numbers into perspective, the reaction probability for  $CH_4$  decomposing on pyrolytic carbon<sup>14</sup> is  $1.5 \times 10^{-8}$  at 1438 K, with a roughly similar reaction probability for

$C_2H_6$ <sup>15</sup>. Based on these data, the value required here for  $R_{CH_4}$  appears quite reasonable while that for  $R_{C_2H_6}$  does not. On the other hand, a high value for  $R_{CH_3}$  is plausible, as  $CH_3$  is a radical.  $X_{C_2H_4}$  and especially  $X_{C_2H_2}$  are so small that these species can be excluded from further consideration.

Although  $X_{CH_3}$  and  $X_{C_2H_6}$  both exceed  $X_{min}$ , we must also consider our second constraint and estimate the rate that  $CH_3$  and  $C_2H_6$  could have been generated from  $CH_4$  decomposition. For purposes of this analysis we will make two extreme assumptions: (1) Every molecule of  $CH_4$  which reacted at all was converted permanently into  $CH_3$  or  $C_2H_6$ . That is, we ignore all reactions such as  $A_{-3}$  which destroyed either species. (2) No matter where in the system these species were formed, they were transported to the crucible for addition to the diamond seed crystals. With these two assumptions we can calculate an upper limit to the rate of diamond growth from  $CH_3$  and  $C_2H_6$ .

Our analysis shows that at steady state approximately 95% of the  $CH_4$  that reacted did so via  $A_3$ , with nearly all the rest reacting via  $A_{-2}$ . Thus, we can calculate the total number of  $CH_4$  molecules reacting/s by evaluating for each  $Z$  the rates of these 2 reactions, shown in Figure 2, multiplying them by the volume element  $dV = AdZ$ , and then integrating with respect to  $Z$ . The result is that the calculated steady state reaction rate integrated over the entire apparatus is  $1.8 \times 10^{14}$   $CH_4$  molecules/s. Since this rate is nearly 500 times lower than that required by our second constraint, we conclude that neither  $CH_3$  nor  $C_2H_6$  (nor any other species) was produced in this system at a rate fast enough to contribute significantly to diamond growth. We infer that diamond growth occurred in this system by direct decomposition of  $CH_4$  on the diamond surface.

It is interesting to compare growth of diamond from  $CH_4$  with growth of pyrolytic carbon from  $C_2H_2$ . The kinetics of the latter reaction can be described using a single Arrhenius expression between 600 and 1700 K with an activation energy of only 25 kcal/mole<sup>16,17</sup>. Since it is unlikely that a reaction involving radicals made from  $C_2H_2$  would have such a low activation energy at 600 K, we expect that the acetylene reaction forming pyrolytic carbon is also a direct molecular decomposition on the carbon surface. It is, however, substantially faster than the decomposition of  $CH_4$  to make pyrolytic carbon or diamond.

As pointed out above, the value we obtained here for  $R_{CH_4}$  is similar to that for  $CH_4$  decomposition on pyrolytic carbon<sup>14,16</sup>. Furthermore, the 55 kcal/mole activation energy measured by Chauhan et al.<sup>7</sup> (or the 58 kcal/mole activation energy measured by Tesner et al.<sup>18</sup> for the same reaction) is similar to the 65 kcal/mole for addition of  $CH_4$  to pyrolytic carbon<sup>17</sup>. Finally, we note that  $H_2$  acts as an inhibitor to growth of both diamond<sup>7</sup> and pyrolytic carbon<sup>14</sup> in  $CH_4$  systems. It is tempting to imagine that diamond and pyrolytic carbon growth are similar processes. If so, we would speculate that diamond—like pyrolytic carbon—can grow from a direct reaction of a variety of hydrocarbons<sup>16</sup>, although the reaction probabilities for different species could vary considerably. Continuing with this line of speculation, the propensity of different growth species to form pyrolytic carbon (rather than diamond) could be different. For example, a molecule such as  $C_2H_2$ , with its multiple bonds, could be more likely to form pyrolytic carbon than  $CH_4$ , which is already  $sp^3$  bonded. (However, even  $CH_4$  does produce pyrolytic carbon.) In that case, since the  $C_2H_2$  concentration increases approximately as the square of the  $CH_4$  concentration when  $CH_4$  is the starting material, we would expect a deterioration in the quality of the diamond films grown with increasing  $CH_4$  concentration. Such a deterioration is in fact observed<sup>2</sup>.

Although one of the main conclusions of this work is that the diamond growth results of Chauhan et al.<sup>7</sup> cannot be accounted for by  $C_2H_2$  or  $CH_3$ , we emphasize that our results do not contradict the calculations of Frenklach and Spear<sup>5</sup> or Tsuda et al.<sup>6</sup>, who claimed that  $C_2H_2$  or  $CH_3$  is the principal growth species in filament- or plasma-assisted diamond film growth. Our results show, instead, that diamond films *can and do* grow from  $CH_4$ , and that neither  $C_2H_2$  nor  $CH_3$  is required. However, given the roughly similar concentrations of  $CH_4$ ,  $CH_3$ ,  $C_2H_4$ , and  $C_2H_2$  under filament-assisted diamond growth conditions<sup>3,4</sup>,  $C_2H_4$ ,  $C_2H_2$  and/or  $CH_3$  could well contribute more than  $CH_4$  to diamond growth there.

Because some of the experimental parameters used in this modeling effort were not measured, we had to make a number of approximations and assumptions. In this section we consider how they affect our conclusions.

The most important approximation is that the temperature and species mole fraction fields were 1-dimensional. In fact, the wall temperatures were stated to be below 473 K, even at the location we have called  $Z = 40$ , where we have assumed a temperature of 1438 K. And we have not accounted for radical destruction which can take place on the walls. Thus, for both temperature and chemical reasons the walls are sinks for radicals. Because of the importance of diffusion in this system, processes which occur at the walls can be expected to have an impact at the crucible, 5 cm away. In our model we can simulate the presence of such a sink 5 cm from the crucible by changing the assumed temperature profile so that it drops to 500 K (instead of 1250 K) by  $Z = 45$ . This results in reductions by factors of 2-3 in  $X_{CH_3}$  and  $X_H$  and factors of 4-6 in  $X_{C_2H_2}$  and  $X_{C_2H_4}$ . By no means does this simple exercise accurately take into account the effect of the walls. What it does show, however, is that the presence of the cool walls lowers the mole fractions of the pyrolysis products (species other than  $CH_4$  and  $H_2$ ). We conclude that the mole fractions shown in Figure 1 are upper limits to their true values, reinforcing our conclusion that no species besides  $CH_4$  could have contributed significantly to diamond growth.

Beyond considering the walls as radical sinks, we have not attempted to model any possible heterogeneous chemistry taking place in this system. We do not expect that extraneous heterogeneous chemistry affected the diamond growth kinetics for three reasons. (1) The rate for pyrolytic carbon growth measured by Chauhan et al.<sup>7</sup> is within a factor of 2 of the rate of pyrolytic carbon growth calculated from the formula of Fedoseev et al.<sup>14</sup> for the same  $CH_4$  and  $H_2$  pressures but in the absence of any diamond. Since this difference is smaller than the experimental uncertainty, we conclude that the presence of diamond has no effect on the growth rate of pyrolytic carbon. Similarly, the analysis of Chauhan et al.<sup>7</sup> shows that the presence of pyrolytic carbon does not affect the growth rate of diamond (except to the extent that it reduces the available diamond surface area). These results make plausible the assumption that extraneous heterogeneous chemistry on the diamond also did not affect the kinetics of diamond growth. (2) The kinetics of diamond growth was the same in flow tubes with hot ( $\sim 1200$  K)<sup>18,19</sup> and cool ( $< 500$  K)<sup>7</sup> walls. We conclude that heterogeneous chemistry on walls of the system did not affect the kinetics of diamond growth. (3) The kinetics of diamond growth was unaffected when platinum, graphite, or quartz were used as crucibles<sup>7,19</sup>. That even a highly active catalytic material such as platinum did not affect the kinetics of diamond growth is perhaps not surprising if the growth species was  $CH_4$ .

## References

1. R.C. DeVries, *Ann. Rev. Mater. Sci.* **17**, 161 (1987).
2. J.C. Angus and C.C. Hayman, *Science* **241**, 913 (1988).
3. (a) F.G. Celli, P.E. Pehrsson, H.-t. Wang, and J.E. Butler, *Appl. Phys. Lett.* **52**, 2043 (1988). (b) F.G. Celli, P.E. Pehrsson, H.-t. Wang, H.H. Nelson, and J.E. Butler, Second Diamond Technology Initiative Symposium, paper W-2, July 13, 1988.
4. S.J. Harris, A.M. Weiner, and T.A. Perry, *Appl. Phys. Lett.*, **53**, 1605 (1988).
5. (a) M. Frenklach and K.E. Spear, *J. Mater. Res.* **3**, 133 (1988). (b) M. Frenklach and K.E. Spear, Second Diamond Technology Initiative Symposium, paper W-8, July 13, 1988.
6. (a) M. Tsuda, M. Nakajima, and S. Oikawa, *J. Am. Chem. Soc.* **108**, 5780 (1986). (b) M. Tsuda, M. Nakajima, and S. Oikawa, *Japanese J. Appl. Phys.* **26**, L527 (1987).
7. a. S.P. Chauhan, J.C. Angus, and N.C. Gardner, *J. Appl. Phys.* **47**, 4746 (1976).  
b. S. P. Chauhan, "Diamond Growth from Vapor at Low Pressurs," Thesis, Chemical Engineering Division, Case Institute of Technology, 1972.
8. G.A. Somorjai, "Principles of Surface Chemistry," Prentice-Hall, New Jersey.
9. (a) M.D. Smooke, *J. Comp. Phys.* **48**, 72 (1982). (b) R.J. Kee, J.F. Grcar, M.D. Smooke, and J.A. Miller, Sandia Report SAND85-8240, 1985.
10. S.J. Harris, A.M. Weiner, R.J. Blint, and J.E.M. Goldsmith, *Twenty-first Symposium (International) on Combustion*, The Combustion Institute, 1033 (1986).
11. S.J. Harris, A.M. Weiner, and R.J. Blint, *Combust. Flame* **72**, 91 (1988).
12. R.J. Kee, F.M. Rupley, and J.A. Miller, Sandia Report SAND87-8215, 1987.
13. (a) D.R. Stull, E.F. Westrum, and G.C. Sinke, *Chemical Thermodynamics of Organic Compounds*, Wiley, New York, 1969; (b) A. Burcat in *Combustion Chemistry* (W.C. Gardiner, Ed.), Springer-Verlag, New York, 1984, p. 455.
14. D.V. Fedoseev, S.P. Vnukov, and V.P. Varnin *Dokl. Akad. Nauk* **218**, 399 (1974).
15. D.V. Denisevich and P.A. Tesner, *Dokl. Akad. Nauk* **212**, 660 (1973).
16. S.J. Harris and A.M. Weiner, *Ann. Rev. Phys. Chem.* **36**, 31 (1985).
17. E.F. Aref'eva, I.S. Rafal'kes, and P.A. Tesner, *Khimiya Tverdogo Topliva (Solid Fuel Chemistry)* **11**, 113 (1977).
18. P.A. Tesner, A.E. Gorodetskii, E.V. Denisevich, A.P. Zakhorov, and T.V. Tehunova, *Dokl. Akad. Nauk* **222**, 1384 (1975).
19. B.V. Derjaguin and D.V. Fedoseev, *Carbon* **11**, 299 (1973).
20. J. Warnatz in *Combustion Chemistry* (W.C. Gardiner, Ed.), Springer-Verlag, New York, 1984, p. 197.
21. D.B. Olson and W.C. Gardiner, *Combust. Flame* **32**, 151 (1978).
22. (a) J.E. Butler, J.W. Fleming, L.P. Goss, and M.C. Lin, in "Laser Probes for Combustion Chemistry," ACS Symposium Series **134**, 397 (1980). (b) P. Glarborg, J.A. Miller, and R.J. Kee, *Combust. Flame* **65**, 177 (1986).
23. W.J. Pitz and C.K. Westbrook, *Combust. Flame* **63**, 113 (1986).

Table I

## Methane/Hydrogen mechanism

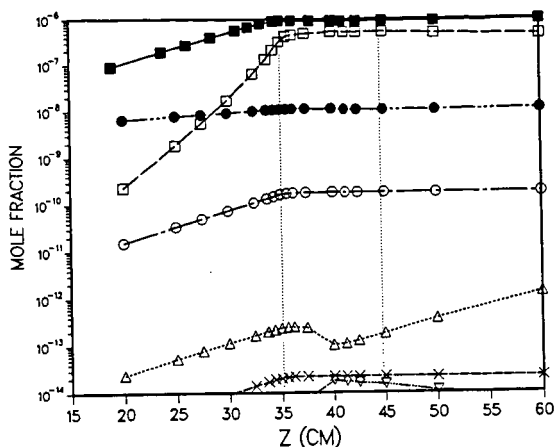
REACTIONS	A	n	E <sub>a</sub>	Ref
A1) $H + H + M = H_2 + M$	9.7E+16	-0.6	0.0	20
A2) $CH_3 + H + M = CH_4 + M$	8.0E+26	-3.0	0.0	20 <sup>a</sup>
A3) $CH_4 + H = CH_3 + H_2$	2.2E+04	3.0	8.8	20
A4) $CH_4 + CH_2 = CH_3 + CH_3$	1.0E+13	0.0	0.0	21
A5) $CH_3 + CH_3 = C_2H_5 + H$	8.0E+14	0.0	26.5	20
A6) $CH_3 + H = CH_2 + H_2$	7.2E+14	0.0	15.1	21
A7) $CH_3 + CH_2 = C_2H_4 + H$	2.0E+13	0.0	0.0	21
A8) $CH_3 + M = CH_2 + H + M$	1.0E+16	0.0	90.6	20
A9) $CH_2 + H = CH + H_2$	4.0E+13	0.0	0.0	20
A10) $CH + CH_4 = C_2H_4 + H$	6.0E+13	0.0	0.0	22
A11) $CH + CH_3 = C_2H_3 + H$	3.0E+13	0.0	0.0	22
A12) $C_2H_6 + H = C_2H_5 + H_2$	5.4E+02	3.5	5.2	20 <sup>b</sup>
A13) $C_2H_6 + CH_3 = C_2H_5 + CH_4$	5.5E-01	4.0	8.3	20 <sup>b</sup>
A14) $C_2H_6 + M = CH_3 + CH_3 + M$	1.0E+19	0.0	68.0	20 <sup>b</sup>
A15) $C_2H_5 + M = C_2H_4 + H + M$	1.0E+17	0.0	31.0	20 <sup>b</sup>
A16) $C_2H_5 + CH_3 = C_2H_4 + CH_4$	7.9E+11	0.0	0.0	23
A17) $C_2H_4 + M = C_2H_2 + H_2 + M$	2.6E+17	0.0	79.4	20 <sup>b</sup>
A18) $C_2H_4 + M = C_2H_3 + H + M$	2.6E+17	0.0	96.6	20
A19) $C_2H_4 + H = C_2H_3 + H_2$	1.5E+14	0.0	10.2	20
A20) $C_2H_4 + CH_3 = CH_4 + C_2H_3$	4.2E+11	0.0	11.2	20
A21) $C_2H_3 + H = C_2H_2 + H_2$	2.0E+13	0.0	0.0	20
A22) $C_2H_3 + M = C_2H_2 + H + M$	3.0E+15	0.0	32.0	20
A23) $C_2H_3 + CH_3 = C_2H_2 + CH_4$	7.9E+11	0.0	0.0	23
A24) $C_2H_2 + M = C_2H + H + M$	4.0E+16	0.0	107.0	20
A25) $C_2H_2 + H = C_2H + H_2$	6.0E+13	0.0	23.7	20

$k = AT^n e^{-E_a/RT}$ ,  $R = 1.99 \times 10^{-3}$  kcal/mole-deg

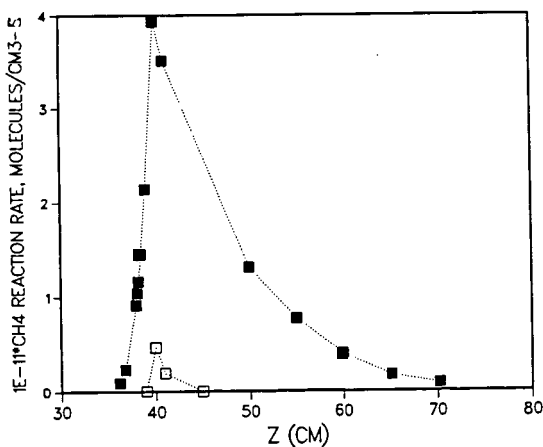
Units are cm<sup>3</sup>, moles, seconds, kilocalories

<sup>a</sup> Results at  $Z = 40$  are more sensitive to the value of this rate constant than to any other rate constant.

<sup>b</sup> Results at  $Z = 40$  show significant sensitivity to the value of this rate constant.



1.  $\log_{10}$  of mole fractions of all species calculated to have mole fractions of at least  $10^{-14}$ . The vertical dotted lines indicate the location of the reaction chamber; the crucible holding the diamond seed crystals is at  $Z = 40$  cm. Solid squares,  $C_2H_6$ ; open squares,  $CH_3$ ; solid circles,  $H$ ; open circles,  $C_2H_4$ ; triangles,  $C_2H_5$ ; crosses,  $C_2H_2$ ; inverted triangles,  $CH_2$ .  $CH_4$  and  $H_2$ , with mole fractions of 0.7 and 0.3, respectively, are not shown.



2. Molecules of  $CH_4$  which reacted/ $cm^3 \cdot s$  as a function of  $Z$ . Solid squares, Reaction  $A_1$ :  $CH_4 + H \rightarrow CH_3 + H_2$ . Open squares, Reaction  $A_{-2}$ :  $CH_4 + M \rightarrow CH_3 + H + M$ . For this analysis these reactions are considered only in the direction indicated by the arrows.